

Notes

Metal Control of the Reaction Site in Reactions of $[(\eta^5\text{-C}_5\text{H}_3)_2(\text{SiMe}_2)_2]\text{M}_2(\text{CO})_4(\mu\text{-H})]^+$ (M = Fe, Ru, Os) with Nucleophilic Amines

Maxim V. Ovchinnikov,[‡] Xiaoping Wang,[†] Arthur J. Schultz,[†]
 Ilia A. Guzei,^{‡,§} and Robert J. Angelici^{*,‡}

Department of Chemistry, Iowa State University, Ames, Iowa 50011, and IPNS,
 Argonne National Laboratory, Argonne, Illinois 60439-4814

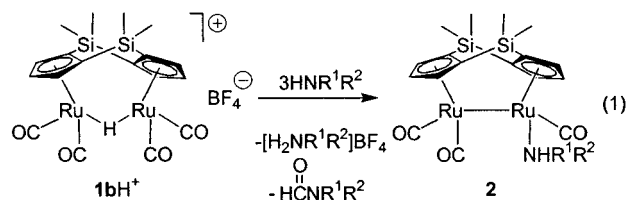
Received February 26, 2002

Summary: Complexes $[(\eta^5\text{-C}_5\text{H}_3)_2(\text{SiMe}_2)_2]\text{M}_2(\text{CO})_4(\mu\text{-H})^+\text{BF}_4^-$ (M = Fe, Ru, Os; **1a**–**1c**), which feature a protonated metal–metal bond, were synthesized. While the Fe and Os complexes react with nucleophilic amines (ammonia, MeNH₂, Me₂NH, Et₃N, morpholine) to give the deprotonated complexes $[(\eta^5\text{-C}_5\text{H}_3)_2(\text{SiMe}_2)_2]\text{M}_2(\text{CO})_4$, the Ru complex reacts with amines by undergoing attack at a CO ligand. These differences in reactivity can be understood by considering the CO ligands in the Ru complex to be more electrophilic than those in the analogous Fe and Os complexes, as indicated by the $\nu(\text{CO})$ values. Molecular structures of **1a**–**1c**, as determined by X-ray diffraction studies, and $[(\eta^5\text{-C}_5\text{H}_3)_2(\text{SiMe}_2)_2]\text{Ru}_2(\text{CO})_4(\mu\text{-H})^+\text{OTf}^-$ (**1b**), as determined by a neutron diffraction study, show that the bridging hydride ligand is sterically concealed and therefore slow to undergo deprotonation upon reaction with bases.

Introduction

Transition metal hydrides have attracted a considerable amount of attention because they are important components of many catalytic and stoichiometric reactions.¹ The acidities of transition metal mono- and polyhydrides depend on the electronic and steric properties of the complexes.² It has also been noted³ that there may be significant differences in the thermodynamic

acidities (equilibrium for proton transfer) and kinetic acidities (the rate of proton transfer) of transition metal hydrides. We recently reported⁴ the synthesis of the protonated dinuclear complex $[(\eta^5\text{-C}_5\text{H}_3)_2(\text{SiMe}_2)_2]\text{Ru}_2(\text{CO})_4(\mu\text{-H})^+\text{BF}_4^-$ (**1b**), whose carbon monoxide ligands are activated to attack by amine nucleophiles (eq 1)



because of the positive charge on the complex and the slow rate of deprotonation of the bridging hydride by the amines. The unusually low kinetic acidity of **1b** was explained by the bulkiness of the dimethylsilyl linkers of the $(\eta^5\text{-C}_5\text{H}_3)_2(\text{SiMe}_2)_2$ ligand and the rigidity of the molecule. Herein we report a comparative investigation of **1b** and its Fe and Os analogues, which lead to a more complete understanding of the low kinetic acidity of **1b** as compared with its reactions with amines that lead to nucleophilic attack on its CO ligands (eq 1).

Experimental Section

General Procedures. All reactions were performed under an argon atmosphere in reagent grade solvents, using standard Schlenk or drybox techniques.⁵ Hexanes, methylene chloride, and diethyl ether were purified by the Grubbs method prior to use.⁶ All other solvents were purified by published methods.⁷ Chemicals were purchased from Aldrich Chemical Co., unless otherwise mentioned, or prepared by literature methods, as referenced below. Alumina (neutral, activity I, Aldrich) was

* To whom correspondence should be addressed. E-mail: angelici@iastate.edu.

[‡] Department of Chemistry, Iowa State University.

[†] Argonne National Laboratory.

[§] Molecular Structure Laboratory, Iowa State University.

[§] Current address: Department of Chemistry, University of Wisconsin, Madison, WI 53706.

(1) (a) Kristjánssdóttir, S. S.; Norton, J. R. In *Transition Metal Hydrides: Recent Advances in Theory and Experiments*; Dedieu, A., Ed.; VCH: New York, 1991; Chapter 10. (b) Pearson, R. G. *Chem. Rev.* **1985**, *85*, 41. (c) Martinho-Simões, J. A.; Beauchamp, J. L. *Chem. Rev.* **1990**, *90*, 629. (d) Bullock, R. M. *Comments Inorg. Chem.* **1991**, *12*, 1.

(2) (a) Angelici, R. J. *Acc. Chem. Res.* **1995**, *28*, 52. (b) Edidin, R. T.; Sullivan, J. M.; Norton, J. R. *J. Am. Chem. Soc.* **1987**, *109*, 3945. (c) Moore, E. J.; Sullivan, J. M.; Norton, J. R. *J. Am. Chem. Soc.* **1986**, *108*, 2257. (d) Jordan, R. F.; Norton, J. R. *J. Am. Chem. Soc.* **1982**, *104*, 1255.

(3) (a) Darensbourg, M. Y.; Ludvig, M. M. *Inorg. Chem.* **1986**, *25*, 2894. (b) Hanckel, J. M.; Darensbourg, M. Y. *J. Am. Chem. Soc.* **1983**, *105*, 6979. (c) Kristjánssdóttir, S. S.; Moody, A. E.; Weberg, R. T.; Norton, J. R. *Organometallics* **1988**, *7*, 1983.

(4) (a) Ovchinnikov, M. V.; Angelici, R. J. *J. Am. Chem. Soc.* **2000**, *122*, 6130. (b) Ovchinnikov, M. V.; Guzei, I. A.; Angelici, R. J. *Organometallics* **2001**, *20*, 691.

(5) Errington, R. J. *Advanced Practical Inorganic and Metalorganic Chemistry*, 1st ed.; Chapman & Hall: New York, 1997.

(6) Pangborn, A. B.; Giardello, M. A.; Grubbs, R. H.; Rosen, R. K.; Timmers, F. J. *Organometallics* **1996**, *15*, 5, 1518.

(7) Perrin, D. D.; Armarego, W. L. F.; Perrin, D. R. *Purification of Laboratory Chemicals*, 2nd ed.; Pergamon: New York, 1980.

degassed under vacuum for 12 h and treated with Ar-saturated water (7.5% w/w). ^1H and ^{13}C NMR spectra were recorded on a Bruker DRX-400 spectrometer using deuterated solvents as internal references. Solution infrared spectra were recorded on a Nicolet-560 spectrometer using NaCl cells with 0.1 mm spacers. Elemental analyses were performed on a Perkin-Elmer 2400 series II CHNS/O analyzer. Syntheses of $\mathbf{1bH}^+\text{BF}_4^-$ and $\mathbf{1bD}^+\text{TfO}^-$ are reported elsewhere.^{4b}

Synthesis of $\{(\eta^5\text{-C}_5\text{H}_3)_2(\text{SiMe}_2)_2\}\text{Fe}_2(\text{CO})_4$ (1a**).** The synthesis of **1a** was adapted and improved from the literature method.⁸ A mixture of $\text{Fe}_2(\text{CO})_9$ (2.00 g, 5.49 mmol) and $(\text{C}_5\text{H}_4)_2(\text{SiMe}_2)_2$ (0.71 g, 2.86 mmol) in toluene (100 mL) was heated to reflux for 32 h. The resulting brown precipitate was removed by filtration, and the brownish green solution was reduced to dryness. The remaining dark solid was chromatographed on an alumina column (5 × 20 cm) first with hexanes and then with a 1:10 (v/v) mixture of CH_2Cl_2 and hexanes, which eluted an emerald-green band containing **1a**. Evaporation gave **1a** as a brown solid (1.80 g, 70%). ^1H NMR (400 MHz, C_6D_6): δ 0.23 (s, 6 H, Si(CH_3)), 0.41 (s, 6 H, Si(CH_3)), 4.31 (t, $J = 2.2$ Hz, 2 H, Cp- H), 4.66 (d, $J = 2.2$ Hz, 4 H, Cp- H). ^{13}C NMR (100 MHz, C_6D_6): δ -3.13 (CH_3), 4.00 (CH_3), 82.84, 92.61, 94.48 (Cp); the CO resonance was not observed. IR (hexanes): $\nu(\text{CO})$ (cm^{-1}) 2015 (vs), 1961 (s). IR (solid on Teflon film): $\nu(\text{CO})$ (cm^{-1}) 1982 (vs), 1942 (s), 1770 (s). Anal. Calcd for $\text{C}_{18}\text{H}_{18}\text{O}_4\text{Fe}_2\text{Si}_2$: C, 46.37; H, 3.89. Found: C, 46.25; H, 3.99.

Synthesis of $\{[(\eta^5\text{-C}_5\text{H}_3)_2(\text{SiMe}_2)_2]\text{Fe}_2(\text{CO})_4(\mu\text{-H})\}^+\text{BF}_4^-$ (1aH}^+\text{BF}_4^-**).** A green solution of **1a** (100 mg, 0.21 mmol) in CH_2Cl_2 (20 mL) was treated with $\text{HBF}_4\cdot\text{Et}_2\text{O}$ (28 μL , 0.25 mmol) at room temperature. A dark purple precipitate of **1aH}^+\text{BF}_4^-** was obtained in nearly quantitative yield (107 mg, 92%) by diluting the solution with a 10-fold excess of ether (200 mL). ^1H NMR (400 MHz, CD_2Cl_2): δ -29.47 (s, 1 H, Fe- H), 0.62 (s, 6 H, Si(CH_3)), 0.75 (s, 6 H, Si(CH_3)), 5.15 (t, $J = 2.0$ Hz, 2 H, Cp- H), 5.84 (d, $J = 2.0$ Hz, 4 H, Cp- H). ^{13}C NMR (100 MHz, CD_2Cl_2): δ -3.50 (CH_3), 2.07 (CH_3), 81.73, 96.38, 98.27 (Cp), 210.04 (CO). Anal. Calcd for $\text{C}_{18}\text{H}_{19}\text{BF}_4\text{O}_4\text{Fe}_2\text{Si}_2$: C, 39.02; H, 3.46. Found: C, 38.63; H, 3.20.

Synthesis of $\{(\eta^5\text{-C}_5\text{H}_3)_2(\text{SiMe}_2)_2\}\text{Os}_2(\text{CO})_4$ (1c**).** A mixture of $\text{Os}_3(\text{CO})_{12}$ (1.00 g, 1.10 mmol), $(\text{C}_5\text{H}_4)_2(\text{SiMe}_2)_2$ (179 mg, 0.73 mmol), and methylisobutyl ketone (4 mL) in decane (100 mL) was heated at 150 °C for 72 h. The black solution was filtered and chromatographed on an alumina column (5 × 20 cm) first with hexanes and then with a 1:10 (v/v) mixture of CH_2Cl_2 and hexanes, which eluted a pale yellow band containing **1c** (yellow solid; 187 mg, 35%). ^1H NMR (400 MHz, CD_3NO_2): δ 0.31 (s, 6 H, Si(CH_3)), 0.53 (s, 6 H, Si(CH_3)), 5.73 (d, $J = 2.0$ Hz, 4 H, Cp- H), 6.00 (t, $J = 2.0$ Hz, 2 H, Cp- H). IR (hexanes): $\nu(\text{CO})$ (cm^{-1}) 2008 (vs), 1940 (s).

Synthesis of $\{[(\eta^5\text{-C}_5\text{H}_3)_2(\text{SiMe}_2)_2]\text{Os}_2(\text{CO})_4(\mu\text{-H})\}^+\text{BF}_4^-$ (1cH}^+\text{BF}_4^-**).** A yellow solution of **1c** (100 mg, 136 mmol) in CH_2Cl_2 (20 mL) was treated with $\text{HBF}_4\cdot\text{Et}_2\text{O}$ (16 μL , 149 mmol) at room temperature. A yellow precipitate of **1cH}^+\text{BF}_4^-** was obtained in nearly quantitative yield (112 mg, 95%) by diluting the solution with a 10-fold excess of ether (200 mL). ^1H NMR (400 MHz, CD_3NO_2): δ -20.80 (s, 1 H, Os- H), 0.54 (s, 6 H, Si(CH_3)), 0.67 (s, 6 H, Si(CH_3)), 6.23 (t, $J = 2.0$ Hz, 2 H, Cp- H), 6.34 (d, $J = 2.0$ Hz, 4 H, Cp- H). ^{13}C NMR (100 MHz, CD_3NO_2): δ -2.80 (CH_3), 2.46 (CH_3), 85.92, 97.98, 99.19 (Cp), 175.09 (CO). Anal. Calcd for $\text{C}_{18}\text{H}_{19}\text{BF}_4\text{O}_4\text{Os}_2\text{Si}_2\text{-CH}_2\text{Cl}_2$: C, 25.14; H, 2.33. Found: C, 25.62; H, 2.38.

X-ray and Neutron Diffraction Structural Studies. X-ray diffraction data for **1aH}^+\text{BF}_4^-**, **1bH}^+\text{BF}_4^-**, and **1cH}^+\text{BF}_4^-** were collected on a Bruker CCD-1000 diffractometer. The structures were solved using direct methods and standard difference map techniques and refined by full matrix least-

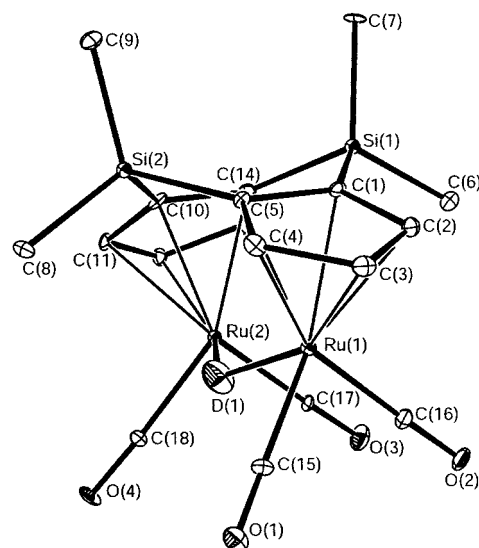


Figure 1. Molecular structure of $\mathbf{1bD}^+\text{TfO}^-$ as determined by neutron diffraction. Thermal ellipsoid drawing, with 50% probability ellipsoids, of $\{[(\eta^5\text{-C}_5\text{H}_3)_2(\text{SiMe}_2)_2]\text{Ru}_2(\text{CO})_4(\mu\text{-D})\}^+$ in $\mathbf{1bD}^+\text{TfO}^-$ showing the labeling scheme. Selected bond distances [\AA] and angles [deg] are as follows: Ru(1)–Ru(2), 3.103(3); Ru(1)–D(1), 1.741(4); Ru(2)–D(1), 1.768(5); Ru(1)–C(15), 1.909(4); Ru(1)–C(16), 1.889(4); Ru(2)–C(17), 1.904(4); Ru(1)–C(18), 1.910(4); Ru(1)–Cp(centroid), 1.880(2); Ru(2)–Cp(centroid), 1.877(3); $\angle\text{Ru}(1)\text{-D}(1)\text{-Ru}(2)$, 124.3(3); $\angle\text{C}(15)\text{-Ru}(1)\text{-D}(1)$, 80.2(2); $\angle\text{C}(16)\text{-Ru}(1)\text{-D}(1)$, 96.4(2); $\angle\text{C}(15)\text{-Ru}(1)\text{-C}(16)$, 89.3(2); $\angle\text{C}(17)\text{-Ru}(2)\text{-D}(1)$, 100.4(2); $\angle\text{C}(18)\text{-Ru}(2)\text{-D}(1)$, 77.4(2); $\angle\text{C}(17)\text{-Ru}(2)\text{-C}(18)$, 91.0(2); $\angle\text{C}(16)\text{-Ru}(1)\text{-Ru}(2)\text{-C}(17)$, 0.25(19); $\angle\text{C}(15)\text{-Ru}(1)\text{-Ru}(2)\text{-C}(18)$, 2.75(19); $\angle\text{Cp(centroid)\text{-Ru}(1)\text{-Ru}(2)\text{-Cp(centroid)}$, 1.3(2); $\angle\text{Cp}\text{-Cp}$ fold angle (angle between the planes of the Cp rings), 131.1(1).

squares procedures using SHELXTL.¹⁰ All hydrogen atoms were placed in the structure factor calculations at idealized positions.

Neutron diffraction data were collected from a single crystal of $\mathbf{1bD}^+\text{TfO}^-$ at the Intense Pulsed Neutron Source (IPNS), Argonne National Laboratory. The IPNS single-crystal diffractometer (SCD) is a time-of-flight (TOF) instrument with a time- and position-sensitive detector.¹¹ A wavelength-dependent spherical absorption correction was applied with $\mu(\lambda) = 0.908 + 0.582\cdot\lambda$ cm^{-1} . Symmetry related reflections were not averaged because of the wavelength dependence of extinction. A total of 4209 independent reflections were used in the structural refinement. The structure was refined with the program SHELXL97.¹² In the final least-squares cycle, carbon, oxygen, fluorine, and hydrogen atoms were refined with anisotropic temperature factors. The remaining heavy atoms were refined isotropically. Final R1 = 0.084, wR2 = 0.156 (for observed data with $I > 2\sigma(I)$).

Results and Discussion

In the structure of complex $\{[(\eta^5\text{-C}_5\text{H}_3)_2(\text{SiMe}_2)_2]\text{Ru}_2(\text{CO})_4(\mu\text{-H})\}^+\text{BF}_4^-$ (**1bH}^+\text{BF}_4^-**) (Figure 1, Table 1), the two Ru atoms are bridged by the doubly linked dicyclopentadienyl ligand.¹³ The most important struc-

(10) All software and sources of the scattering factors are contained in the SHELXTL (version 5.1) program library (G. Sheldrick, Bruker Analytical X-Ray Systems, Madison, WI).

(11) Schultz, A. J. *Trans. Am. Cryst. Assoc.* **1993**, *29*, 29.

(12) Sheldrick, G. M. *SHELXL-97. A program for crystal structure refinement*, Release 97-2; Institut für Anorganische Chemie der Universität: Göttingen, Germany, 1998.

(8) Siemeling, U.; Jutzki, P.; Neumann, B.; Stammler, H. G.; Hursthouse, M. B. *Organometallics* **1992**, *11*, 1328.

(9) Hiermeier, J.; Koehler, F. H.; Mueller, G. *Organometallics* **1991**, *10*, 1787.

Table 1. Crystallographic Data for $1aH^+BF_4^-$, $1bH^+BF_4^-$, $1cH^+BF_4^-$ (X-ray diffraction) and $1bD^+TfO^-$ (neutron diffraction)

	$1aH^+BF_4^-$	$1bH^+BF_4^-$	$1cH^+BF_4^-$	$1bD^+TfO^-$
formula	$C_{18}H_{19}BF_4Fe_2O_4Si_2$	$C_{18}H_{19}BF_4O_4Ru_2Si_2 \cdot \frac{1}{2}CH_2Cl_2$	$C_{18}H_{19}BF_4O_4Os_2Si_2 \cdot \frac{1}{2}CH_2Cl_2$	$C_{19}H_{18}D_1F_3O_7Ru_2S_1Si_2$
fw	554.02	686.92	871.19	707.73
cryst syst	tetragonal	orthorhombic	monoclinic	monoclinic
space group	$\bar{I}4$	$Cmca$	$C2/m$	$P2_1/n$
a, Å	22.0019(11)	13.9174(7)	18.8021(8)	11.750(2)
b, Å	22.0019(11)	18.7899(9)	13.8847(6)	15.488(3)
c, Å	9.6504(5)	18.5989(9)	9.8502(4)	13.194(2)
α , deg	90	90	90	90
β , deg	90	90	109.8492(10)	92.67(1)
γ , deg	90	90	90	90
V, Å ³	4671.6(4)	4863.7(4)	2418.73(18)	2416.7(7)
Z	8	8	4	4
cryst color, habit	purple block	yellow prism	yellow block	yellow block
cryst size, mm	0.40 × 0.10 × 0.10	0.40 × 0.26 × 0.20	0.50 × 0.20 × 0.10	2.80 × 1.40 × 0.80
$\mu(Mo, K\alpha)$, mm ⁻¹	1.398	1.501	10.761	
temp, K	173(2)	173(2)	173(2)	20
abs corr	empirical	empirical	empirical	
θ range	1.85 to 26.36°	2.12 to 28.29°	1.86 to 26.37°	
no. of reflns collected	17803	15540	10413	4209
no. of indep reflns	4758 [$R(int) = 0.0250$]	2960 [$R(int) = 0.0359$]	2578 [$R(int) = 0.0365$]	3605
$R(F)$ ($I \geq 2\sigma(I)$) ^a	$R1 = 0.0252$, wR2 = 0.0641	$R1 = 0.0306$, wR2 = 0.0773	$R1 = 0.0213$, wR2 = 0.0590	$R1 = 0.084$, wR2 = 0.156

$$^a R1 = \sum ||F_o| - |F_c|| / \sum |F_o|, wR2 = \{ \sum [w(F_o^2 - F_c^2)^2] / \sum [w(F_o^2)^2] \}^{1/2}.$$

tural distinctions between complex $1bH^+BF_4^-$ and the corresponding deprotonated complex $\{(\eta^5-C_5H_3)_2(SiMe_2)_2\}-Ru_2(CO)_4$ ¹⁴ (**1b**) are (a) the longer Ru–Ru distance in $1bH^+BF_4^-$ (3.1210(5) Å) compared to that in **1b** (2.8180(3) Å), (b) the larger $\angle Cp-Cp$ fold angle (defined as the angle between the two Cp planes) in $1bH^+BF_4^-$ (131.1(1)°) compared to that in **1b** (122.86°), as expected for the longer Ru–Ru distance in $1bH^+BF_4^-$, and (c) the eclipsed CO groups ($\angle C(16)-Ru(1)-Ru(2)-C(17)$, 0.25(19)°) in $1bH^+BF_4^-$, but staggered CO groups in **1b** ($\angle C-Ru-Ru-C$, 32.3°).¹⁵ The X-ray structure refinement suggests that the bridging hydride ligand in $1bH^+BF_4^-$ is not in the plane defined by Ru(1), Ru(2), and the centroids of the two Cp rings. Because the location of this hydride, as deduced from X-ray data, has a large uncertainty, a neutron diffraction study of $1bD^+TfO^-$ was undertaken.^{16,17} The neutron diffraction data clearly establish the “off-center” position of the bridging hydride, which is reflected in the angle (112.3°) between the Cp(centroid)–Ru(1)–Ru(2)–Cp(centroid) and Ru(1)–D(1)–Ru(2) planes (Figure 1). The “off-center” site of the hydride ligand is also supported by a long C(15)···C(18) distance (4.089 Å) compared to the much shorter C(16)–C(17) distance (3.031 Å). The

(13) Crystallographic data (excluding structure factors) for the structures in this paper have been deposited with the Cambridge Crystallographic Data Centre as supplementary publication no. CCDC-163489 ($1aH^+BF_4^-$), CCDC-163488 ($1bH^+BF_4^-$); X-ray diffraction), CCDC-163102 ($1bD^+TfO^-$; neutron diffraction), CCDC-163490 ($1cH^+BF_4^-$). Copies of the data can be obtained, free of charge, on application to CCDC, 12 Union Road, Cambridge CB2 1EZ, UK (fax: +44 1223 336033 or e-mail: deposit@ccdc.cam.ac.uk).

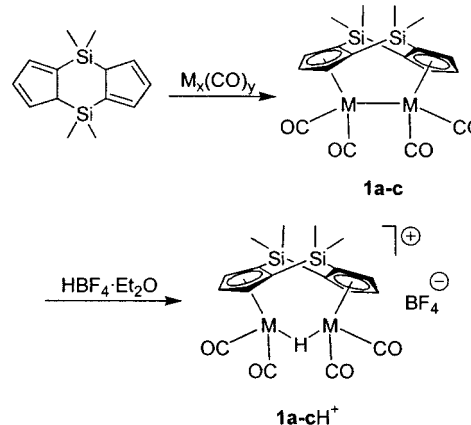
(14) Ovchinnikov, M. V.; Klein, D. P.; Choi, M.-G.; Guzei, I. A.; Angelici, R. J. *Organometallics* **2002**, *21*, 617.

(15) Similar trends were reported for protonated and deprotonated complexes $\{(\eta^5-C_5H_3)_2(SiMe_2)_2\}W_2(CO)_6$ and $\{(\eta^5-C_5H_3)_2(SiMe_2)_2\}W_2(CO)_6(\mu-H)^+$. See: McKinley, S. G.; Angelici, R. J.; Choi, M.-G. *Organometallics* **2002**, *21*, 1235.

(16) Deuterated complex $\{(\eta^5-C_5H_3)_2(SiMe_2)_2\}Ru_2(CO)_4(\mu-D)^+TfO^-$ ($1bD^+TfO^-$) was used in order to simplify the refinement of the neutron diffraction data.

(17) For a recent review on neutron diffraction studies of transition metal hydrides, see: Bau, R.; Drabnis, M. H. *Inorg. Chim. Acta* **1997**, *259*, 27.

Scheme 1. Syntheses of Complexes **1a–c** and $1a-cH^+BF_4^-$ (M = Fe (a), Ru (b), Os (c))



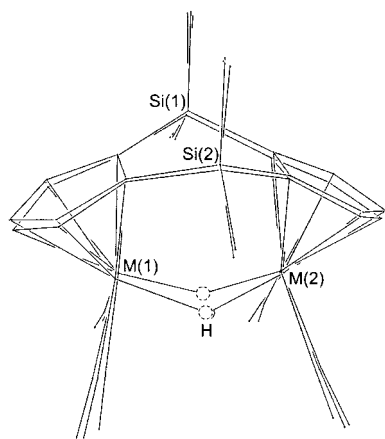
bridging hydride ligand is located above (toward the SiMe₂ group) the C(15)–Ru(1)–Ru(2)–C(18) plane, as indicated by the angle (20.66°) between this plane and the Ru(1)–D(1)–Ru(2) plane. The “off-center” location may be controlled by the tendency of both Ru atoms to adopt a pseudo-octahedral geometry, with angles of approximately 90° between the adjacent carbonyls and the Ru–H–Ru bond, and at the same time achieve a relatively short Ru–Ru distance. The bridging hydride is fluxional in solution, as inferred from the ¹H and ¹³C NMR spectra, which show, even at −50 °C, only two signals for the Si(CH₃)₂ methyl groups in accord with the rapid movement of the bridging hydride ligand from one side to the other of the Ru–Ru vector. On the other hand, the solid-state ¹³C NMR spectrum of $1bH^+BF_4^-$ exhibits four signals (δ 0.26 br, 2.73, 8.63) for the Si(CH₃)₂ methyl groups and 10 partially overlapped Cp resonances (δ 91.79–111.34 range), as expected for the solid-state structure.

Complexes $1aH^+BF_4^-$ and $1cH^+BF_4^-$, the Fe and Os analogues of $1bH^+BF_4^-$, were synthesized as shown in Scheme 1. The structures (X-ray crystallography) and

Table 2. Selected Properties of $[(\eta^5\text{-C}_5\text{H}_3)_2(\text{SiMe}_2)_2]\text{M}_2(\text{CO})_4(\mu\text{-H})^+$ **1a**- cH^+BF_4^- and **1bD** $^+\text{TfO}^-$ (M = Fe (**a**), Ru (**b**), Os (**c**))

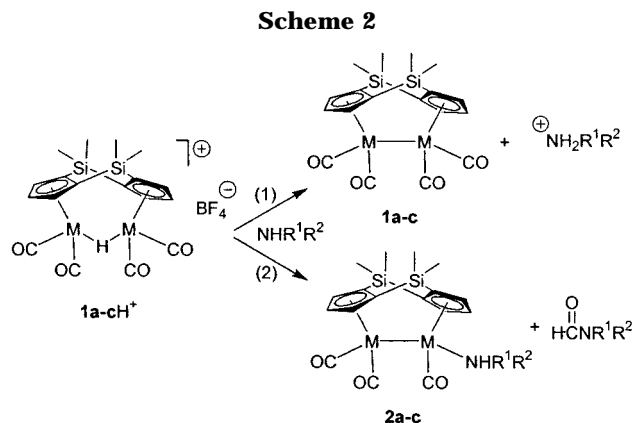
	1aH $^+\text{BF}_4^-$	1bH $^+\text{BF}_4^-$ ^a	1bD $^+\text{TfO}^-$ ^b	1cH $^+\text{BF}_4^-$
M–M, Å	2.999(7)	3.1210(5)	3.103(3)	3.0933(3)
M–H, Å	1.601, 1.660	1.728(5)	1.741(4), 1.768(5)	
C(16)⋯C(17), Å	2.935	3.053	3.031	2.982
C(15)⋯C(18), Å	3.695	4.139	4.089	4.118
$\nu(\text{CO})$, cm^{-1} (CH_2Cl_2)	2069 (vs), 2039 (w), 2025 (s)	2077 (vs), 2050 (w), 2027 (s)	2077 (vs), 2050 (w), 2027 (s)	2067 (vs), 2036 (w), 2011 (s)
average $\nu(\text{CO})$, cm^{-1}	2044	2051	2051	2038

^a Structural parameters are obtained from X-ray diffraction data. ^b Structural parameters are obtained from neutron diffraction data.

**Figure 2.** Overlay of the structures of **1aH** $^+\text{BF}_4^-$, **1bD** $^+\text{TfO}^-$, and **1cH** $^+\text{BF}_4^-$, illustrating the similarities in their molecular structures.

spectroscopic (NMR, IR) characteristics (Table 2, Figure 2) of **1aH** $^+\text{BF}_4^-$ and **1cH** $^+\text{BF}_4^-$ are very similar to those of **1bH** $^+\text{BF}_4^-$. The “off-center” location of the bridging hydride in **1aH** $^+\text{BF}_4^-$ and **1cH** $^+\text{BF}_4^-$ is evident from the unsymmetrical positions of the CO ligands, similar to that observed in **1bH** $^+\text{BF}_4^-$, although the bridging hydride ligand is not located in the X-ray study of **1cH** $^+\text{BF}_4^-$. The location of the bridging hydride inside the rigid cavity created by the CO ligands and the $\text{Si}(\text{CH}_3)_2$ groups (Figures 1, 2) suggests that complexes **1a,cH** $^+\text{BF}_4^-$ should also undergo deprotonation by basic amines very slowly; as a result, their CO ligands should be susceptible to nucleophilic attack. Surprisingly, compounds **1a,cH** $^+\text{BF}_4^-$ react with amines (ammonia, MeNH_2 , Me_2NH , Et_3N , morpholine) to yield only the deprotonated complexes **1a,c**. There was no evidence for nucleophilic attack on CO, such as formation of formamides or complexes of type **2** (Scheme 2), although Et_3N deprotonates the **1a,cH** $^+\text{BF}_4^-$ complexes slowly ($t_{1/2} \approx 21$ h in CDCl_3).

To understand why **1bH** $^+\text{BF}_4^-$ reacts with primary and secondary amines by attack at a CO ligand (eq 1) while **1aH** $^+\text{BF}_4^-$ and **1cH** $^+\text{BF}_4^-$ undergo simple deprotonation with the same amines, it is necessary to consider both the relative rates of deprotonation (path 1, Scheme 2) and nucleophilic attack on the CO ligands (path 2). The rate of deprotonation, i.e., the kinetic acidity, is similar for all three complexes **1a–cH** $^+\text{BF}_4^-$. All of the complexes **1a–cH** $^+\text{BF}_4^-$ undergo complete deprotonation in $\text{DMSO}-d_6$ solution, where the $\text{DMSO}-d_6$ is both the solvent and the base ($\text{p}K_a(\text{H}_2\text{O}) = -1.8$),¹⁸ at approximately the same rate ($t_{1/2} \approx 7.5$ h). On the other hand, the rate of nucleophilic attack on a CO ligand depends on the electrophilicity of the CO group.



The relative electrophilicities of the CO ligands in **1a–cH** $^+\text{BF}_4^-$ may be estimated from their average $\nu(\text{CO})$ values.¹⁹ The higher $\nu(\text{CO})$ value for the Ru complex **1bH** $^+\text{BF}_4^-$ (average $\nu(\text{CO}) = 2051$ cm^{-1}) indicates that its CO ligands are more electrophilic than those in its Fe and Os analogues (average $\nu(\text{CO}) = 2044$, 2038 cm^{-1} respectively, Table 2). Thus, it is reasonable that **1bH** $^+\text{BF}_4^-$ reacts with primary and secondary amines by nucleophilic attack on a CO ligand (path 2); only a small amount of deprotonation (path 1) occurs.^{4,20} On the other hand, the observation that **1aH** $^+$ and **1cH** $^+$ react with amines to give only deprotonation products (path 1) is consistent with a slower rate of amine attack on the CO ligand, as expected for these complexes with lower $\nu(\text{CO})$ values. Thus, it is the electronic activation of the CO ligands by Ru in **1bH** $^+$ that leads to products resulting from nucleophilic attack on CO.

In conclusion, we have demonstrated that a CO ligand in the protonated complex $[(\eta^5\text{-C}_5\text{H}_3)_2(\text{SiMe}_2)_2]\text{Ru}_2(\text{CO})_4(\mu\text{-H})^+$ (**1bH** $^+\text{BF}_4^-$) is the site of reaction with amines because of the high electrophilicity of the CO ligands and the low kinetic acidity of the bridging hydride—a unique combination of kinetic properties that are not found in the Fe and Os analogues.

Acknowledgment. This research was supported by the NSF (CHE-9816342 to R.J.A.). The work at Argonne was supported by the U.S. Department of Energy, Office of Basic Energy Sciences-Materials Sciences, under Contract No. W-31-109-ENG-38.

(18) Perrin, D. D. *Dissociation Constants of Organic Bases in Aqueous Solution*; Butterworth: London, 1972.

(19) (a) Angelici, R. J. *Acc. Chem. Res.* **1972**, *5*, 335. (b) Jolly, W. L.; Avanzino, S. C.; Rietz, R. R. *Inorg. Chem.* **1977**, *16*, 964.

(20) It is interesting to note that the rates of MeO^- attack on CO ligands of $\text{M}(\text{CO})_5$ decrease with the metal in the order $\text{Os} > \text{Ru} > \text{Fe}$, even though the $\nu(\text{CO})$ values for the Ru complex are higher than those of the Os and Fe complexes. Trautman, R. J.; Gross, D. C.; Ford, P. C. *J. Am. Chem. Soc.* **1985**, *107*, 2355.

Supporting Information Available: Complete details of the crystallographic study of **1a**H⁺BF₄⁻, **1b**H⁺BF₄⁻, **1c**H⁺BF₄⁻ (X-ray diffraction), and **1d**D⁺TfO⁻ (neutron diffraction) and tables giving crystallographic data for **1a**H⁺BF₄⁻, **1b**H⁺BF₄⁻, **1c**H⁺BF₄⁻, and **1d**D⁺TfO⁻ including atomic coordinates,

bond lengths and angles, and anisotropic displacement parameters are available free of charge via the Internet at <http://pubs.acs.org>.

OM020167W